Determination of the Parameters in a Model for the Magnetic Losses in Silicon Steel Sheets

Carlos L. B. Silva[1], Adalberto J. Batista[2]

[1]Escola de Engenharia Elétrica e de Computação, Universidade Federal de Goiás, Goiânia, Brazil, carlosleandro82@gmail.com
[2]Escola de Engenharia Elétrica e de Computação, Universidade Federal de Goiás, Goiânia, Brazil, batista@eee.ufg.br

Abstract: This paper describes an experimental procedure for determination of the parameters involved in a magnetic losses prediction model in silicon steel sheets. The employed model was developed for sinusoidal and non-sinusoidal magnetic induction waveforms without local minima, which implies in the absence of minor loops in the major B-H loop. Experimental results are presented in order to validate the model.

Index terms: Silicon steel, losses modeling, hysteresis loss, classical loss, residual loss.

1. INTRODUCTION

Soft magnetic materials, such as silicon steel and ferrites, have been widely applied to magnetic core construction in electrical machinery, transformers and inductors as well as in other electrical components and equipments. The design of those equipments and components depends on the magnetic characteristics of these materials, and it is important to the designer having access to reliable and general information. However, it has been noticed manufacturers usually do not provide magnetic material characteristics in a generalized form, that is, in graphical form and in mathematical models, where would be possible to identify, for instance, the effects of the sample temperature and magnetic induction waveform, including its amplitude and frequency.

In spite of the present applications and the continuously arising of a diversity of applications where the magnetic induction is non-sinusoidal, manufacturers of silicon steel have not provided general information even for sinusoidal magnetic-induction. Such information would have allowed the designers not only to improve the design of the referred equipments and electrical components but also optimize them considering energy efficiency, volume, weight etc. Furthermore, it would allow the material manufacturers controlling the quality of their products and the information about them.

In order to contribute to filling this gap and strengthening the Brazilian Test Laboratory Network in this area, an automated measurement system for the characterization of soft magnetic materials, called SCaMMa, has been implemented [1,2]. In the present stage of development, this system allows obtaining the B-H loop, the initial magnetization curve, the normal permeability and the magnetic losses in silicon steel and ferrites. During the measurement procedure, the magnetic induction waveform (sinusoidal or non-sinusoidal) and sample temperature are controlled. Having in mind the restrictions of the equipments and materials used in the system, the characterization of silicon steel sheets is feasible for the following tipical ranges: 20 ºC to 85 ºC; 3 Hz to 5 kHz and 0.4 T to 1.8 T.

The silicon steel magnetic characterization through SCaMMa can be performed with either the Epstein frame [3] or the so called Single Sheet Tester (SST) [4] as magnetic characterization device.

The goal of this work is to present the fundamental aspects related to the experimental determination of the parameters involved in a magnetic losses prediction model in silicon steel sheets [5-7]. Experimental results, obtained via SCaMMa and a 25 cm Epstein frame, are presented in order to validate the model and illustrate the features and potentialities of this system.

2. THE MEASUREMENT SYSTEM

Figure 1(a) presents a schematic diagram of the proposed system using a 25 cm Epstein frame as magnetic characterization device. Figure 2(b) shows this Epstein frame.

The equipments of the SCaMMa are completely controlled by computer through a GPIB bus (*General Purpose Interface Bus)*. Thus, some specific software functions, called Virtual Instruments (VI), were developed in LabVIEW environment [8], in order to support the system [11]. Moreover, some other VI were implemented to deal with functions such as system setup, signal data acquisition, mathematical processing of the quantities regarded to the magnetic characterization, essay report generation and result preview graphic interfaces. Therefore, once the system is suitably started, the operator will be able to follow all the magnetic characterization of the sample step-by-step through a computer.

During the measurement process, the sample is demagnetized and both temperature and magnetic- induction waveform at the sample are controlled according to system setup adjusted by the operator. Only after the control process convergence on each point are the voltages sampled and the quantities regarded to the magnetic characterization computed. The results are dynamically shown to the system operator during the process.

Recently, our laboratory has participated in an interlaboratory comparison program of the INMETRO (Brazil) Mate-

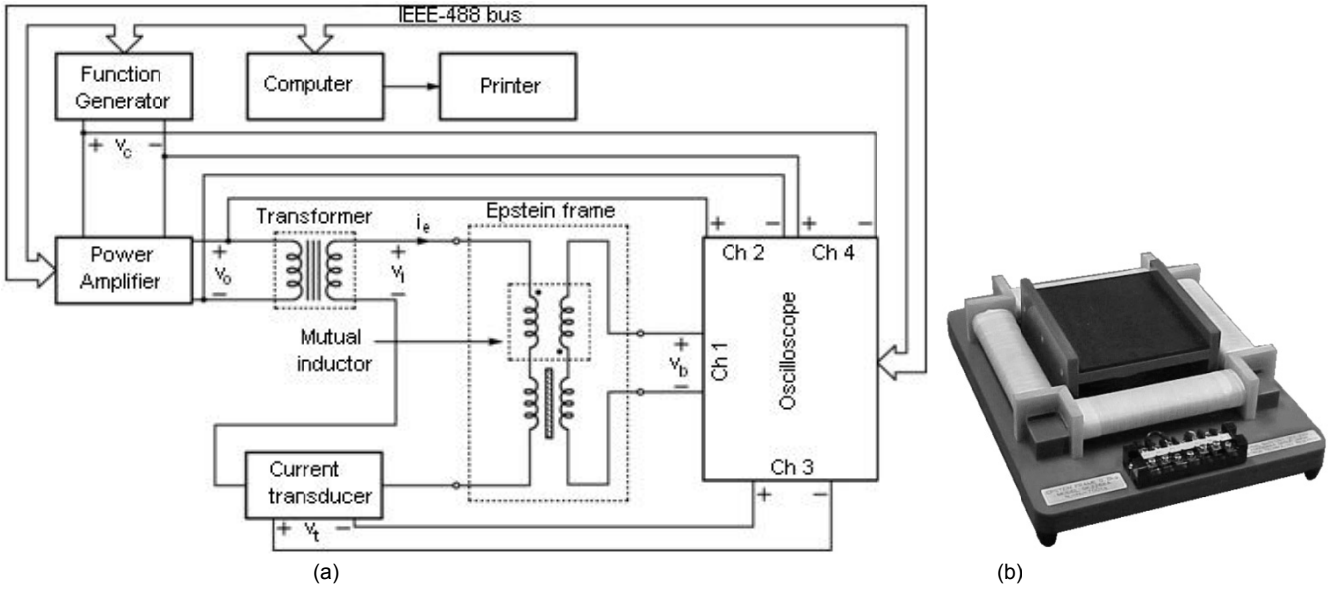

Fig. 1. (a) SCaMMa schematic diagram using the 25 cm Epstein frame; (b) 25 cm Epstein frame.

rials Metrology Division (DIMAT). The magnetic characterization at the DIMAT Laboratory of Magnetism is performed with a Brockhaus System MPG100D hysteresis tracer, whose measurements are traceable to the PTB (Germany) through a certified reference material. The participants of this program were asked to measure the total magnetic loss in non-oriented grain silicon steel sheets at 1.0 T, 1.3 T and 1.5 T and at 50 Hz and 60 Hz, by using a 25 cm Epstein frame. As a result, the greatest diference obtained with SCaMMa was 1.1 %.

3. THE MAGNETIC LOSSES MODEL

The total energy dissipated per magnetization cycle and per magnetic material volume unit corresponds to the area of the B-H loop. This energy can be specified in J/kg, as the ratio of its obtained value to the material density. In the present model for the losses calculation, the energy is obtained under specific conditions of temperature and excitation. The model relies on the physically based idea of loss separation, where the total energy dissipated per cycle under the referred specific conditions is expressed as the sum of the hysteresis (or quasi-static loss), classical (or eddy current loss), and residual (or excess loss) components according to (1) [5-7].

$$W = W_h + W_{cl} + W_{res} \tag{1}$$

With

$$W_h = \frac{P_{fh}}{f_h} \tag{2}$$

$$W_{cl} = \frac{\sigma d^2}{12 f m_v} \frac{1}{T} \int_0^T \left(\frac{dB}{dt} \right)^2 dt \tag{3}$$

$$W_{res} = \frac{1}{f m_v} \sqrt{\sigma G V_0 S} \frac{1}{T} \int_0^T \left| \frac{dB}{dt} \right|^{1.5} dt \tag{4}$$

Where:

W - Dissipated total energy per magnetization cycle due to the total magnetic loss [J/kg]

W_h - Dissipated energy per magnetization cycle due to the hysteresis loss [J/kg]

W_{cl} - Dissipated energy per magnetization cycle due to the classical loss [J/kg]

W_{res} - Dissipated energy per magnetization cycle due to the residual loss [J/kg]

P_{fh} - Magnetic loss measured at the quasi-static frequency [W/kg]

f_h - Quasi-static frequency [Hz]

σ - Material electric conductivity [Ω/m]

d - Sheet thickness [m]

m_v - Material density [kg/m^3]

f - Frequency [Hz]

T - Period [s]

$B(t)$ - Magnetic induction in the sample [T]

G - Dimensionless coefficient

V_0 - Parameter that characterizes the statistical distribution of the local internal fields (A/m)

S - Sheet transversal section area [m^2]

The magnetic field, $H(t)$, and the magnetic-induction, $B(t)$, at the material under test are calculated according to (5) and (6).

$$H(t) = \frac{N_e i_e(t)}{l_e} \tag{5}$$

$$B(t) = \frac{1}{N_b A_e} \left[\int_0^t v_b(t)dt - \frac{1}{nT} \int_0^{nT} \left(\int_0^t v_b(t)dt \right) dt \right] \tag{6}$$

Where:

$H(t)$ - Magnetic field in the sample [A/m]

N_e - Epstein frame primary number of turns

$i_e(t)$ - Epstein frame primary current[A]

l_e - Average length of the magnetic path [m]

N_b - Epstein frame secondary number of turns

A_e - Cross section area of the sample set [m^2]

$v_b(t)$ - Epstein frame secondary voltage [V]

n - Number of periods

The second term in (6) yields the cancellation of the average value of the magnetic-induction produced by a non-zero initial value.

The total magnetic loss is calculated according to (7).

$$W = \frac{1}{m_v}\int_0^T H(t)\left(\frac{dB}{dt}\right)dt \tag{7}$$

with

$$\frac{dB(t)}{dt} = \frac{1}{N_b A_e} v_b(t) \tag{8}$$

The present model uses the Bertotti's statistical theory of losses concerning the residual loss [6,7]. In this theory, Bertotti introduced the concept of magnet object in such a way that the dissipated energy per cycle, due to the residual loss, is affected by the statistic distribution of the local internal fields caused by each simultaneously active magnetic object, as described by the parameter V_0 in (4).

3.1 Magnetic loss for sinusoidal magnetic induction waveform

The magnetic induction sinusoidal regime is an important particular case in the magnetic loss modeling study, since the determination of the parameter V_0 is made in this regime. The used procedure is described as follow.

It is considered the sinusoidal magnetic induction waveform of amplitude B_p and frequency f, as given by (9).

$$B(t) = B_p sen(2\pi f t) \tag{9}$$

The substitution of (9) in (3) and (4) results in the equation for the calculation of the dissipated energy per cycle under sinusoidal magnetic induction waveform:

$$W_{sen}(f) = W_h + \frac{\sigma\pi^2 d^2}{6m_v} B_p^2 f + \frac{8.76}{m_v}\sqrt{\sigma G V_0 S}\; B_p^{1.5}\sqrt{f} \tag{10}$$

Equation (10) gives the value of the dissipated energy per cycle under sinusoidal magnetic induction as a function of its amplitude and frequency and characteristic parameters related to the sample geometry and material (σ, d, m_v, G, V_0 e S). In fact, the parameter G is constant and equal to 0.1356 [6,7].

The energy associated to the hysteresis loss, W_h, has to be obtained in a frequency as low as possible and, in this case, the B-H loop is called hysteresis loop or quasi-static B-H loop. In the absence of minor loops in the major B-H loop, that is, when the magnetic induction waveform does not possess local minima, it is assumed that this energy is independent of magnetic induction waveform and frequency; however it depends on the peak value of the magnetic induction [5-7]. Therefore, since the value of B_p was defined for which W_h was determined, the parameter V_0 will be the only unknown quantity in (10).

In order to determine the value of V_0 from (10) it is necessary to measure the total energy per magnetization cycle at test frequencies different from the quasi-static frequency. From (10), one can observes that, for a given B_p, V_0 can be determined from the slope of the best straight fitting line described by ΔW as a function of $f^{1/2}$, as given by (11). In fact, if V_0 is determined by using just one test frequency then, for a given B_p, the relative error of the model presents a tendency to increase with either the decreasing or the increasing of the frequency relative to the referred test frequency.

$$\Delta W = W_h + \frac{8.76}{m_v}\sqrt{\sigma G V_0 S}\; B_p^{1.5}\sqrt{f} \tag{11}$$

with

$$\Delta W = W - W_{cl} = W_{sen}(f) - \frac{\sigma\pi^2 d^2}{6m_v} B_p^2 f \tag{12}$$

3.2. Magnetic loss for trapezoidal magnetic induction waveform

The magnetic induction trapezoidal regime results from the application of a PWM (Pulse Width Modulation) voltage waveform to the magnetic device winding. The PWM voltage term is referred to the series of n_p pulses (in half cycle) of amplitude V_p, as can be seen in Figure 2. This kind of voltage waveform is commonly generated by static electronic converters, which are used in several applications such as, for instance, electrical motor variable speed driving. For this reason this waveform was choosen for illustrate the validity of the model.

It is worth to note from Figure 2 that the resulting magnetic induction waveform is trapezoidal. The magnetic induction increases at a constant rate when $v(t) = V_p$, does not change when $v(t) = 0$ and decreases at a constant rate when $v(t) = -V_p$. The duration of the i-th pulse is τ_i. Therefore, in the trapezoidal regime, the derivative of the magnetic induction with respect to the time can be written as:

$$\begin{aligned} &\frac{dB}{dt} = 0 && t : v(t) = 0 \\ &\frac{dB}{dt} = \pm\frac{2B_p}{n_p \sum_{i=1}^{} \tau_i} && t : v(t) = \pm V_p \end{aligned} \tag{13}$$

The substitution of (13) in (3) e (4) results in the equation for the calculation of the dissipated energy per cycle under trapezoidal magnetic induction waveform:

$$W_{trap}(f) = W_h + \frac{2\sigma d^2}{3m_v}\frac{B_p^2}{n_p \sum_{i=1}^{} \tau_i} + \frac{1}{m_v}\sqrt{\sigma G V_0 S}\;\frac{4\sqrt{2}B_p^{1.5}}{\left(n_p \sum_{i=1}^{} \tau_i\right)^{0.5}} \tag{14}$$

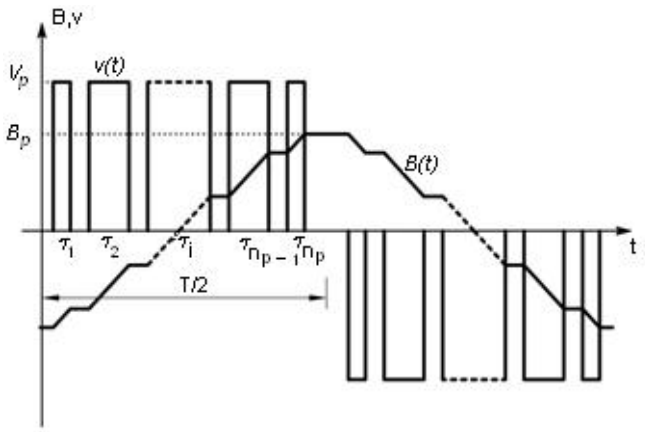

Fig 2. PWM voltage and its resulting magnetic induction.

The duty cycle, α, of the PWM voltage corresponds to the percentage of the half-cycle in which the value of the instantaneous voltage is non-null. Then,

$$\alpha = 2f \sum_{i=1}^{n_p} \tau_i \tag{15}$$

Thus, the dissipated energy per cycle in the trapezoidal magnetic induction waveform is written as a function of f and α:

$$W_{trap}(f) = W_h + \frac{4\sigma d^2}{3m_v} \frac{B_p^2 f}{\alpha} + \frac{1}{m_v}\sqrt{\sigma G V_0 S}\,\frac{8B_p^{1.5}\sqrt{f}}{\sqrt{\alpha}} \tag{16}$$

4. EXPERIMENTAL RESULTS

The experimental results presented as follow were obtained for magnetic induction waveforms with B_p equal to 0.4 T, 0.6 T, 0.8 T, 1.0 T, 1.2 T, 1.4 T, and 1.6 T, at a quasi-static frequency, f_h, equal to 5 Hz and at test frequencies, f, equal to 50 Hz, 60 Hz, 100 Hz, 250 Hz, 400 Hz, and 500 Hz. Table 1 shows the characteristics of the material under test, which is the non-oriented grain silicon steel, type E170 manufactured by ACESITA [9]. Table 2 shows the characteristics of the sample used in the measurement. The thickness (d) and the transversal section area (S) were calculated from the length, width and sheet volume, which was obtained from its density and mass [3]. The temperature of the sample was not controlled, since the magnetic losses model does not account for its influence. The ambient temperature was (25,0 ± 3,0) ºC.

Table 1. Material characteristics.

Item	Value
Manufacturer	ACESITA
Designation	E170
Density (m_v)	7.65 g/cm^3
Conductivity (σ)	2.22 x 10^6 Ω/m

Table 2. Sample characteristics.

Item	Value
Mass	519 g
Width	30.00 mm
Length	275.22 mm
Transversal section area (S)	127.76 mm^2
Thickness (d)	500.3 μm

4.1. Sinusoidal magnetic induction waveform

Figure 3 shows the experimental results, obtained for sinusoidal magnetic induction waveforms, for ΔW as a function of $f^{1/2}$ superposed to the corresponding curves obtained by curve fitting. Table 3 shows the respective values for the dissipated energy per cycle due to the hysteresis, W_h, and for the parameter V_0. In fact the hysteresis losses at a given B_p were obtained as the intercept of the respective straight fitting line. Figure 4 shows the respective values for the parameter V_0 as a function of B_p superposed to the corresponding curve obtained by curve fitting. Figure 5 shows the respective loss prediction curves superposed to the corresponding experimental results. Table 4 shows the respective relative errors between the predicted and measured values for the total magnetic loss at the test frequencies. Figure 6 illustrates the respective B-H loops for sinusoidal magnetic induction waveforms with B_p equal to 1.2 T and at frequencies equal to 5, 50, 250 and 500 Hz. Figure 7 illustrates the respective B-H loops for sinusoidal magnetic induction waveforms with frequency equal to 60 Hz and at B_p values equal to 0.4 T, 1.0 T, e 1.4 T.

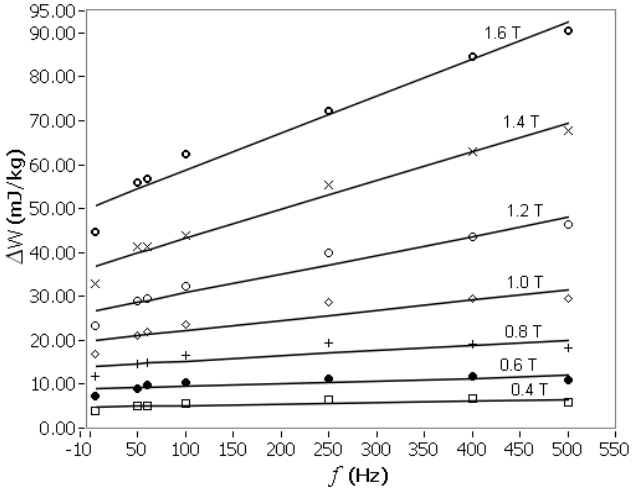

Fig.3. Comparison between predicted and measured values for ΔW under sinusoidal magnetic induction waveform.

Table 3. Experimental values for W_h and V_0.

B_p (T)	W_h (mJ/kg)	V_0
0.4	4.194	0.023
0.6	7.923	0.025
0.8	12.160	0.038
1.0	16.641	0.067
1.2	20.848	0.125
1.4	28.267	0.178
1.6	39.501	0.199

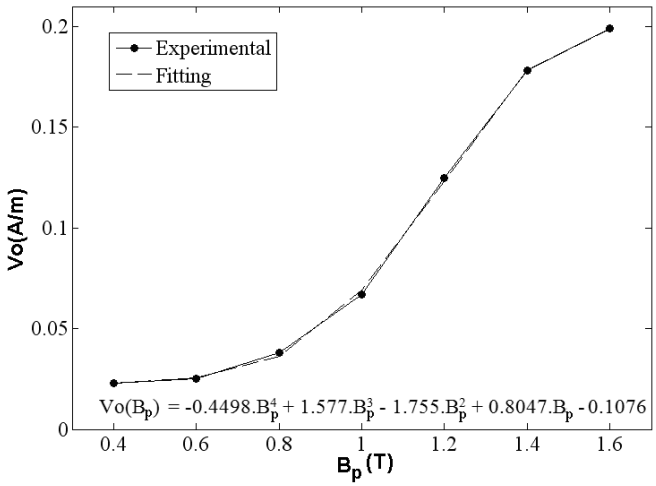

Fig. 4. Parameter model V_0 as a function of B_p.

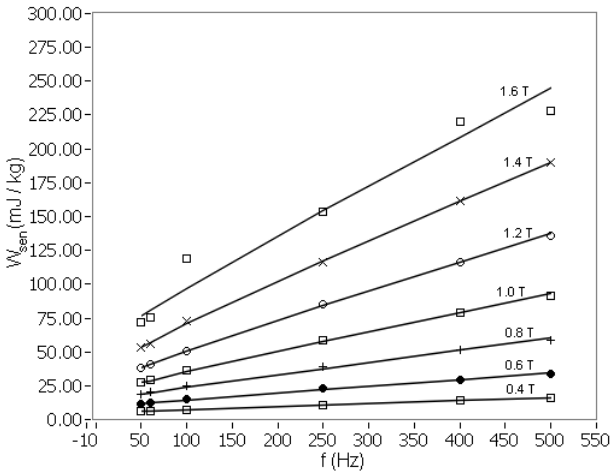

Fig. 5. Comparison between predicted and measured values for the total magnetic loss under sinusoidal magnetic induction waveform.

Table 4. Relative errors between the measured and predicted values for the total magnetic loss under sinusoidal magnetic induction waveform.

Relative error (%)							
f (Hz)	B_p (T)						
	0.4	0.6	0.8	1.0	1.2	1.4	1.6
50	1.40	0.46	-0.32	-0.07	-0.92	-0.52	-6.04
60	0.98	2.91	1.57	1.26	-0.41	-1.26	-7.06
100	5.10	-4.42	3.91	2.51	0.04	2.35	18.48
250	1.29	5.14	3.62	1.40	1.08	-1.21	-0.27
400	1.20	-0.30	0.14	-0.23	0.004	-0.26	5.28
500	-3.04	-3.59	-2.81	1.27	-0.83	-0.01	-7.39

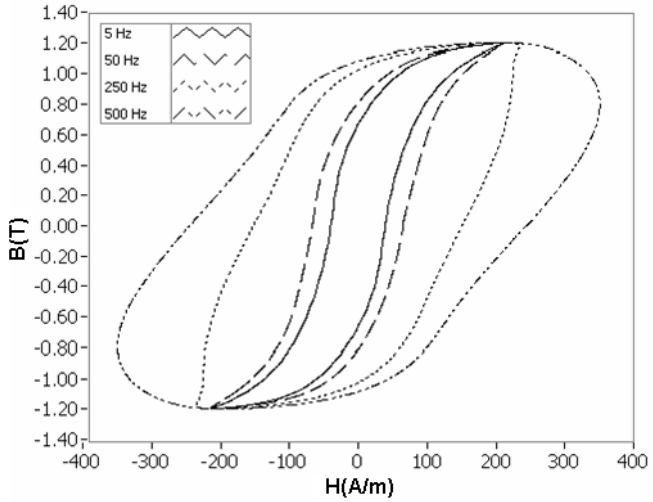

Fig. 6. B-H loops obtained under sinusoidal magnetic induction waveforms at a fixed B_p value and different frequencies.

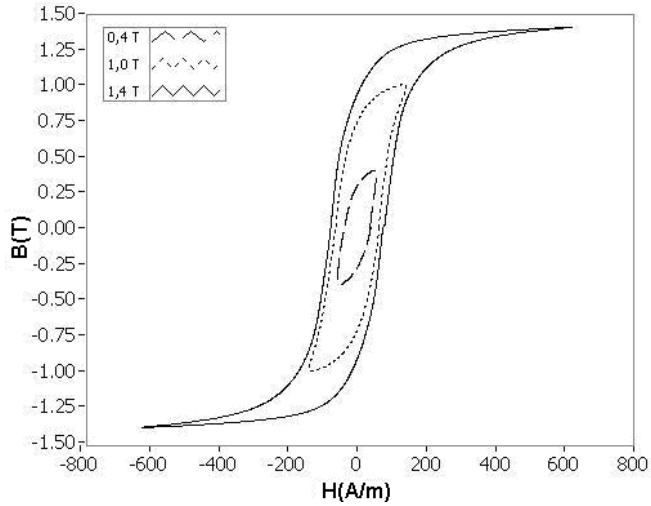

Fig. 7. B-H loops obtained under sinusoidal magnetic induction waveforms at a fixed frequency and different B_p values.

4.2. Trapezoidal magnetic induction waveform

The results presented in this section were obtained for the magnetic induction trapezoidal regime, resulting from the PWM voltage waveform with three equal pulses in half cycle ($n_p = 3$) and duty cycle $\alpha = 0.5$ in the B-winding of the Epstein frame.

Figure 8 shows the respective loss prediction curves superposed to the corresponding experimental results. Table 5 shows the respective relative errors between the measured and predicted values for the total magnetic loss at the test frequencies. Figure 9 shows the respective B-H loops for trapezoidal magnetic induction waveforms with B_p equal to 1.2 T and at frequencies equal to 20, 100 and 150 Hz. Figure 10 shows the respective B-H loops for trapezoidal magnetic induction waveforms with frequency equal to 60 Hz and at B_p values equal to 0.4 T, 1.0 T, e 1.4 T.

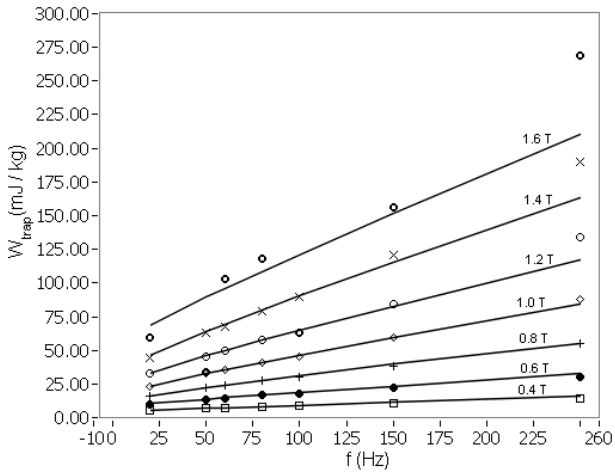

Fig. 8. Comparison between predicted and measured values for the total magnetic loss under trapezoidal magnetic induction waveform.

Table 5. Relative errors between the measured and predicted values for the total magnetic loss under trapezoidal magnetic induction waveform.

Relative error (%)							
f (Hz)	B_p (T)						
	0.4	0.6	0.8	1.0	1.2	1.4	1.6
20	0.39	-1.90	-2.31	0.93	-1.70	-4.05	-14.83
50	-2.88	-1.33	-1.34	0.21	-0.82	-1.97	-165.43
60	-3.27	-2.03	-0.88	0.11	-0.44	-2.95	6.75
80	-0.90	-1.52	-0.85	-0.80	-0.18	-1.26	7.77
100	-3.00	-4.45	-2.28	-2.01	-2.45	-0.80	-91.10
150	-4.88	-7.71	-4.66	0.77	1.95	4.38	3.16
250	-12.81	-6.41	-0.19	4.56	12.48	14.20	21.69

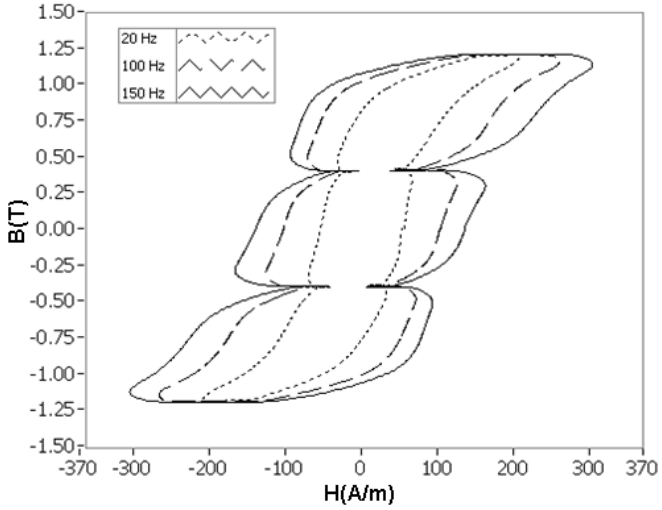

Fig. 9. B-H loops obtained under trapezoidal magnetic induction waveforms at a fixed B_p value and different frequencies.

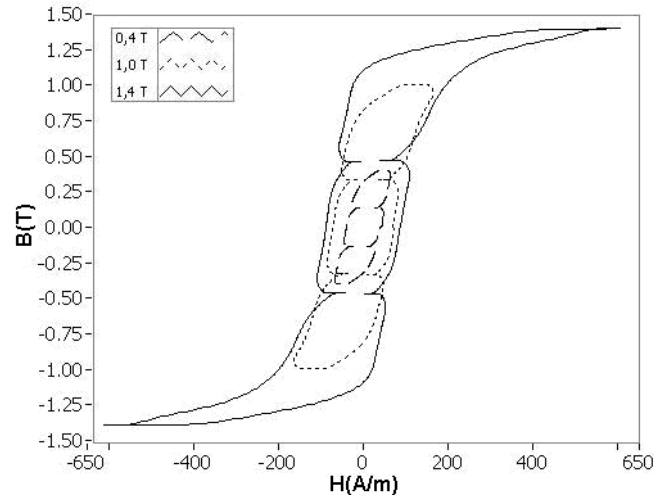

Fig. 10. B-H loops obtained under trapezoidal magnetic induction waveforms at a fixed frequency and different B_p values.

4.3. Discussion

The experimental results presented in this section show that the model could be used with reasonable accuracy for the calculation of the magnetic loss under different magnetic induction waveforms. However, there are limits of applicability of this model in terms of the maxima magnetic induction amplitude and frequency. From Figures 5 and 8 and Tables 4 and 5, one can observes that: a) the model presents a reasonable accuracy up to 1.4 T, independently of the magnetic induction waveform (without local minima in this case); and b) the frequency limit, beyond which the accuracy of the model is inacceptable, seems to depend on the magnetic induction waveform.

In the model here described, the hysteresis losses, W_h, and the parameter V_o depend on the magnetic induction amplitude at which they were determined and the model is mathematically expressed as a function of the fundamental frequency of the magnetic induction waveform for a given value of B_p. However, for the purpose of equipments and electrical components design, a model expressed as a function of the peak value of the magnetic induction for a given working frequency is more adequate. This can be justified based on the fact that the frequency is, in general, an input data to the design and the designer must establish the optimum peak value of the magnetic induction in order to avoid core saturation or to limit the magnetic losses. In the case where the magnetic induction waveform is sinusoidal or trapezoidal (which occurs as a result from the application of a PWM voltage waveform), a magnetic losses model, expressed as a function of the peak value of the magnetic induction waveform for a given frequency and also based on the loss separation, can be achieved [10]. This model uses four parameters whose identification has been pursued by some authors [11,12]. Two of these parameters are related to the hysteresis losses, k_h and α (which models hysteresis losses according to Steinmetz law), and the other two, k_{cl} and k_{exc}, are related to the classical and excess losses, respectively.

The limits of applicability of the model expressed as a function of the peak value of the magnetic induction for a given working frequency in terms of this peak value also presents a reasonable accuracy up to about 1.2 - 1.4 T.

No definitive explanation has been established in the literature for the causes of the limits of applicability of these models.

Concerning the magnetic losses model expressed as a function of the peak value of the magnetic induction for a given working frequency, a better modeling of the hysteresis losses could be promising [13].

5. CONCLUSION

In this work it was investigated the determination of the parameters in a model for the magnetic losses in silicon steel sheets under sinusoidal and non-sinusoidal magnetic induction waveforms without local minima (that is, in the absence of minor loops in the major B-H loop). In this model the total magnetic loss in the sample is obtained by adding three different components of losses (hysteresis, classical and residual losses). This model includes parameters that can be obtained only experimentally, which causes essential the utilization of a magnetic characterization system.

It was verified that such model could be used with reasonable accuracy for the calculation of the magnetic loss under different magnetic induction waveforms. However, there are limits of applicability of this model in terms of the maxima magnetic induction amplitude and frequency. The results obtained by the authors indicate that, in general, the

model presents a reasonable accuracy up to 1.4 T, independently of the type of silicon steel and waveform of magnetic induction (without local minima in this case). Besides, the frequency limit, beyond which the accuracy of the model is inacceptable, seems to depend on the type of silicon steel and waveform of magnetic induction. In fact this model does not account for the influence of the frequency and temperature on the sample conductivity and for the skin effect. It is expected these aspects, once considered in the model, can lead to its improvement.

There is a version of the present model that is applicable to magnetic induction waveforms with local minima, that is, in the presence of minor loops in the major B-H loop. The authors have been working in the implementation of the respective software in SCaMMa for the determination of the parameters of such model.

REFERENCES

[1] J. P. F. Lima, A. J. Batista, P.C.M. Machado, "Automated Measurement System for Soft Magnetic Materials Characterization-Application to Silicon Steel", proceedings of the XVII Congresso Brasileiro de Engenharia e Ciência dos Materiais, p. 5112-5123, 2006. CD-ROM.

[2] J. P. F. Lima, A. J. Batista, E. G. Marra, "Magnetic-Induction Waveform Control Method Applied to Silicon Steel Characterization", proceedings of the VII International Conference on Industrial Applications, p. 1-8, 2006. CD-ROM.

[3] ASSOCIAÇÃO BRASILEIRA DE NORMAS TÉCNICAS. ABNT NBR 5161: Produtos Laminados Planos de Aço para Fins Elétricos – Verificação das Propriedades. Rio de Janeiro, 1977.

[4] A. J. Batista, J. P. F. Lima, "Numerical Analysis of the Field Distribution in a Single Sheet Tester", proceedings of the MOMAG 2008, p. 320-325, 2008. CD-ROM.

[5] E. Barbisio, F. Fiorillo, C. Ragusa, "Predicting Loss in Magnetic Steels Under Arbitrary Induction Waveform and with Minor Hysteresis Loops", IEEE Trans. on Magnetics, v. 40, n. 4, p. 1810-1819, 2004.

[6] G. Bertotti, "Physical Interpretation of Eddy Current Losses in Ferromagnetic Materials. I. Theoretical Considerations", J. Appl. Phys., v. 57, n. 6, p. 2110-2117, 1985.

[7] G. Bertotti, "General Properties of Power Losses in Soft Ferromagnetic Materials", IEEE Trans. on Magnetics, v. 24, n. 1, p. 621-630, 1988.

[8] NATIONAL INSTRUMENTS. LabVIEW v. 6.1 User Manual, 2002.

[9] ACESITA. Aços Elétricos. 1ª ed., 17 p., 2007. Available in: http://www.acesita.com.br/port/produtos_servicos/silicio_biblioteca.asp. Accessed in: Dec. 12, 2008.

[10] M. Amar, F. Protat, "A Simple Method for the Estimation of Power Losses in Silicon Iron Sheets under Alternating Pulse Voltage Excitation", IEEE Trans. on Magnetics, vol. 30, n. 2, pp. 942-944, 1994.

[11] F. B. R. Mendes, *Análises de Medidas de Perdas Magnéticas em Lâminas de Aço ao Silício*, Santa Catarina, 2004, Dissertação de mestrado, Universidade Federal de Santa Catarina.

[12] C. L. B. Silva, A. J. Batista, "A Genetic Algorithm for Parameters Identification in a Model of Losses in Magnetic Steels", "not published".

[13] F. J. G. LANDGRAF, M. F. CAMPOS; J. Leicht, "Hysteresis loss subdivision", Journal of Magnetism and Magnetic Materials, v. 320, p. 2494-2498, 2008.